Theoretical Calculations of Equilibrium Concentrations for Species Generated in Analytically Important Flames

Larry L. Reigle, William J. McCarthy,[1] and A. Campbell Ling[2]
Department of Chemistry, West Virginia University, Morgantown, W. Va. 26506

The compositions of several flames at various temperatures and differing oxidant/fuel ratios have been determined theoretically by use of an iterative computer technique based on a thermodynamic model. Systems chosen were: acetylene–nitrous oxide, acetylene–oxygen, acetylene–air, hydrogen–nitrous oxide, hydrogen–oxygen, and hydrogen–air. In view of the importance that acetylene–nitrous oxide flames have in contemporary analytical techniques, this particular system has been examined further when containing a metallic vapor. The calculations indicate that the free-atom fractions for aluminum, molybdenum, silicon, titanium, and tungsten vary with the fuel/oxidant ratio, but that copper and iron-free atom fractions remain relatively invariant with changes in flame stoichiometry.

Several methods have been described to estimate the concentrations of various species present in a flame. One approach involves finding a product distribution that will satisfy mass balance criteria and restraints imposed by equilibrium constants for a variety of different reactions *(2, 13)*. A feature of this method is that simplifications may be made by recognizing that some species will be present in very small concentrations, and that the presence of these species is relatively unimportant. However, this method utilizes a set of simultaneous equations to describe the equilibrium processes, and for even moderately complex systems, the set becomes quite formidable. Another method *(16)*, known as the free-energy minimization method, considers all possible gaseous species [condensed species can be handled also *(14)*] that might be produced, but in return, eliminates the need for a full knowledge of relative concentrations and therefore avoids the necessity of deciding which species are the major components in the flame. However, even for this method, practical considerations and/or chemical intuition can lead to substantial reductions in computational times. Results of equilibrium calculations by the free-energy minimization method have been reported by Anderson *(1)*, and by Taylor and co-workers *(3, 4)*. This paper further extends and amplifies these calculations to flames that are of interest to contemporary analytical chemistry, and includes calculations involving seven selected metal vapors to simulate flame spectroscopy involving added analytes.

Experimental

A Fortran IV G program was written for an IBM 360/75 computer based on experimental techniques described by White et al. *(13, 16)* and Oliver et al. *(14)*. The equilibrium concentrations of the n species that comprise the flame system are given in terms of a set of mole numbers $X = x_1, x_2, x_3 \ldots x_n$. The required set X is that one which will conditionally minimize the total free energy of the system subject to overall mass-balance considerations. The total free energy, $G(X)$, can be written as the sum of the chemical potentials, μ_i, for the species i such that

$$G(X) = \sum_{i=1}^{i=n} \mu_i \tag{1}$$

The chemical potential for species i in an ideal gas mixture at a total pressure P can be written in terms of a standard chemical potential μ_i° *(10)* which is pressure independent *(7)*, where

$$\mu_i = x_i\left[\mu_i^\circ + RT \ln P + RT \ln\left(x_i / \sum_{i=1}^{i=n} x_i\right)\right] \tag{2}$$

The determination of the equilibrium composition is then a matter of finding the nonnegative values, x_i, that comprise X and will conditionally minimize Equation 1 subject to the restraint

$$\sum_{i=1}^{i=n} x_i a_{ij} = b_j \; (j = 1, 2, \ldots m) \tag{3}$$

where x_i is the mole number for the ith species, a_{ij} is the number of atoms of element j in the ith species, and b_j is the total original number of atomic weights in the initial mixture. Negative mole numbers generated by the iteration procedure were corrected by redefining a corrected mole number, Z_i, in terms of the newly generated negative term, x_i' and the corresponding positive x_i value from the previous cycle

$$Z_i = x_i' + \lambda|(x_i - x_i')| \tag{4}$$

where λ is computed in such a way as to make all negative mole numbers just positive, and is then used to correct the whole set X of mole numbers. This new nonnegative set is the basis for the next cycle. The iteration procedure was continued until such time as the newly generated mole number $(x_{ult})_i$ did not differ from its value $(x_{penult})_i$ in the preceding cycle by an arbitrarily chosen difference Δ, where

$$\Delta = |(x_{ult})_i - (x_{penult})_i| / |(x_{ult})_i| \tag{5}$$

and Δ was set at 10^{-3}. Major species in the equilibrium calculations of the contributing species formed the input data to a new program which generated visual representations of concentrations as a function of temperature via a Cal-Comp-563 Plotter accessory.

Results

Acetylene flames. Acetylene flames with air, oxygen, and nitrous oxide are used extensively in contemporary analytical chemistry. The acetylene–air flame has the lowest temperatures of the three, and is the most transparent, thus providing a good signal-to-noise ratio for analytes that are easily atomized and which do not form stable compounds at the temperatures prevailing in these

[1]Deceased.
[2]To whom correspondence should be addressed.

Table I. Partial Pressures of Gaseous Components Generated in Nitrous Oxide Acetylene Flames for Various Temperatures and Differing Oxidant/Fuel Ratios[a]

	N_2O/C_2H_2 = 1.40			N_2O/C_2H_2 = 2.00			N_2O/C_2H_2 = 2.60		
Species	2700K	3000K	3300K	2700K	3000K	3300K	2700K	3000K	3300K
C	− 6	− 5	− 4	− 8	− 7	− 5	−11	−10	− 9
CH	− 7	− 5	− 5	− 9	− 7	− 6	−12	−11	−10
CHO	− 5	− 5	− 5	− 5	− 5	− 5	− 6	− 6	− 5
CH_2	− 7	− 6	− 6	− 9	− 8	− 7	−12	−12	−11
CH_3	− 5	− 5	− 5	− 7	− 7	− 7	−11	−11	−11
CH_4	− 6	− 6	− 7	− 8	− 8	− 8	−12	−12	−13
CN	− 4	− 4	− 3	− 6	− 5	− 4	− 9	− 9	− 8
CO[b]	− 1	− 1	− 1	− 1	− 1	− 1	− 1	− 1	− 1
CO_2	− 7	− 7	− 7	− 5	− 5	− 6	− 2	− 2	− 2
C_2	− 7	− 5	− 4	−11	− 9	− 7	−17	−16	−15
C_2H[b]	− 3	− 3	− 2	− 8	− 7	− 5	−14	−14	−13
C_2H_2[b]	− 3	− 2	− 2	− 7	− 7	− 5	−13	−13	−13
C_3	− 6	− 4	− 3	−12	−10	− 8	−21	−20	−19
H[b]	− 2	− 2	− 1	− 2	− 2	− 1	− 2	− 2	− 2
HCN[b]	− 2	− 2	− 2	− 4	− 4	− 3	− 7	− 7	− 7
H_2[b]	− 1	− 1	− 1	− 1	− 1	− 1	− 2	− 2	− 2
H_2O	− 6	− 7	− 7	− 4	− 5	− 6	− 2	− 2	− 2
N	− 7	− 6	− 5	− 6	− 6	− 5	− 6	− 6	− 5
NH	− 7	− 6	− 6	− 7	− 6	− 5	− 7	− 6	− 6
NH_2	− 7	− 7	− 6	− 7	− 7	− 6	− 7	− 7	− 7
NH_3	− 7	− 7	− 6	− 7	− 7	− 6	− 7	− 7	− 7
NO	− 9	− 9	− 8	− 7	− 6	− 7	− 4	− 3	− 3
NO_2	−19	−18	−18	−14	−14	−15	− 9	− 8	− 7
N_2[b]	− 1	− 1	− 1	− 1	− 1	− 1	− 1	− 1	− 1
N_2H_2	−12	−11	−11	−12	−11	−11	−12	−12	−11
N_2O	−13	−13	−13	−11	−11	−11	− 8	− 8	− 7
O	− 9	− 8	− 8	− 7	− 6	− 6	− 4	− 3	− 2
OH	− 8	− 8	− 7	− 6	− 6	− 6	− 3	− 2	− 2
O_2	−15	−14	−14	−10	−10	−11	− 4	− 4	− 3

[a]Temperatures are in K, concentrations are given in terms of log (P/P_o), where P are partial pressures in atmospheres to the nearest power of ten, and P_o = 1 atm. Thermodynamic data taken from Ref. *10*. [b]Major products with $P > 10^{-3}$ atm.

systems. Both C_2H_2/O_2 and C_2H_2/N_2O flames provide higher temperatures that can allow a greater efficiency in free-atom production modes, but the high-burning velocity of the C_2H_2/O_2 flame can lead to turbulence and increased noise, and for this reason C_2H_2/N_2O flames are to be preferred. It should be noted that temperatures in the flame systems vary with both fuel/oxidant ratios and height of the system above the burner tip *(18)*. In view of its importance and widespread use, the C_2H_2/N_2O flame is considered first, and in more detail than the other systems.

Concentrations of contributing species to the C_2H_2/N_2O flame have been calculated for three arbitrarily chosen oxidant/fuel ratios (N_2O/C_2H_2 of 1.40, 2.00, 2.60) and seven arbitrarily chosen temperatures (2700–3300K at increments of 100K) which cover the range of experimentally observed values. Data at 2700, 3000, and 3300K, for all species considered are displayed in Table I for each of the fuel/oxidant ratios. Complete temperature dependences for the major species (partial pressures, 10^{-3} atm) are shown in Figure 1. For fuel-rich flames, especially at the lower temperatures, condensed carbon contributes significantly to the product distribution; the dependences of condensed carbon concentrations at different fuel/oxidant ratios are therefore shown in Figure 2 as the fraction of carbon relative to total initial carbon content. Since the product distribution can be extremely sensitive to fuel/oxidant ratios, the isothermal (2900K) variation in concentration of major products with this variable is shown in Figure 3.

The free atom fraction β for a metallic analyte added to any flame system is defined by

$$\beta = P_M/(P_M + P_{MO} + P_{MO_2} + P_{MOH} + \dots) \quad (6)$$

where P_i refers to the partial pressures of species i, and M, MO, MO_2, and MOH to metallic vapor, metallic oxide, metallic dioxide, and metallic hydroxide, respectively. Free-atom fractions for aluminum, copper, iron, molybdenum, silicon, titanium, and tungsten were calculated for various oxidant/fuel ratios between 1.40 and 2.80 (N_2O/C_2H_2 ratios), and at temperatures from 2700–3000K at 100° intervals (See note following Literature Cited). In general, β showed a regular dependence on temperature, but a very marked dependence on the fuel/oxidant ratio under isothermal conditions (2900K), and this dependence is illustrated graphically by the data in Figure 4. It is obvious from Figure 4 that it is virtually impossible to use N_2O/C_2H_2 ratios greater than ca. 2.2 for the analyses of Si, Ti, Mo, and W, in flame systems and this is discussed later in this paper.

Concentrations of major species generated in various C_2H_2/O_2 flames are shown in Figure 5 as a function of temperature, and condensed carbon concentrations under isothermal conditions (3300K) as a function of fuel/oxidant ratio for this system are shown in Figure 6. The data in Figure 6 demonstrate that C_2H_2/O_2 flames are prone to generate relatively large concentrations of condensed carbon, especially in fuel-rich systems. The changes in concentration of major species as the fuel/

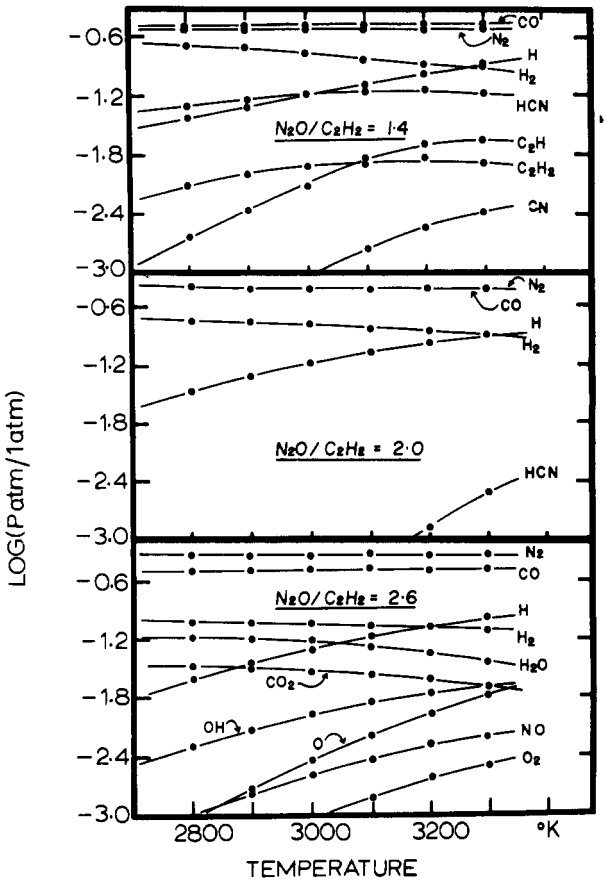

Figure 1. Temperature dependence of concentrations for major species generated in acetylene/nitrous oxide flames at different fuel/oxidant ratios

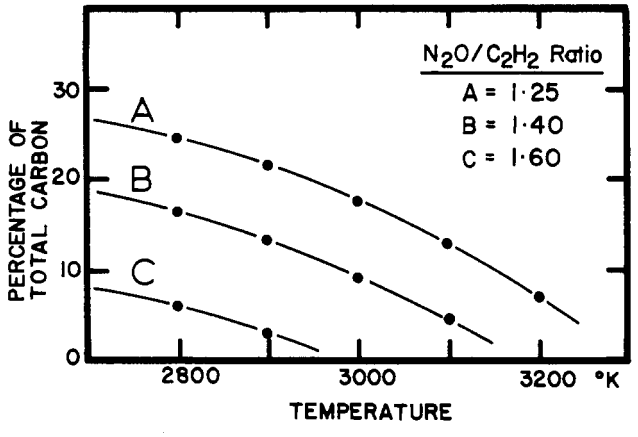

Figure 2. Temperature dependence of condensed carbon concentrations for different fuel/oxidant ratios in acetylene/nitrous oxide flames

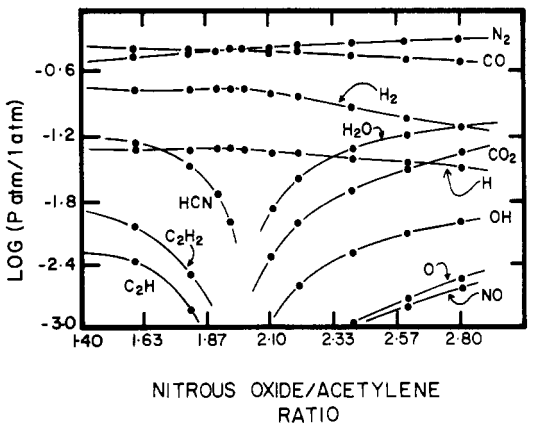

Figure 3. Dependence of concentrations for major species generated in acetylene/nitrous oxide flames on the fuel/oxidant ratio under isothermal conditions (2900K)

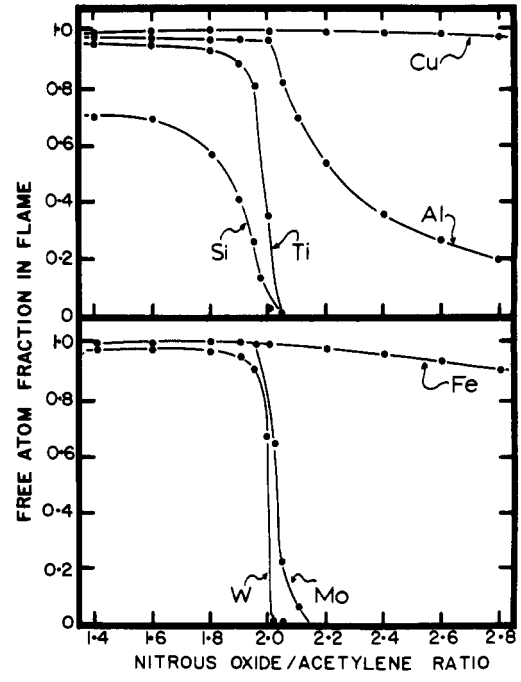

Figure 4. Dependence of free-atom fractions on fuel/oxidant ratio in acetylene/nitrous oxide flames under isothermal conditions (2900K)

oxidant ratio is changed under isothermal conditions (3300K) are shown in Figure 7.

The temperature of C_2H_2/air flames is significantly lower (several hundred degrees) compared to the C_2H_2/O_2 and C_2H_2/N_2O flames considered above. Among other effects, this leads to a large concentration of solid carbon in flames which are fuel-rich, and unless recognized may offset the advantages of a relatively higher transparency and lower flame noise compared to the other two systems. The concentrations of major species present in C_2H_2/air flames are displayed in Figure 8 as a function of temperature, condensed carbon fractions are shown as a function of temperature in Figure 9, and isothermal (2600K) concentrations given as a function of fuel/oxidant ratio in Figure 10.

Hydrogen flames Hydrogen flames are usually supported by either air or oxygen, but the H_2/N_2O flame has been suggested for use in emission studies of easily atomized metals *(17)*. Since hydrogen flames tend to be relatively transparent, they are particularly useful for atomic emission and absorption studies, despite their lower temperatures compared to corresponding acetylene flames. In general, background radiation from the flame is weak with the exception of that from OH bands *(5)*. Even under extremely fuel-rich conditions, hydrogen flames do not exhibit the strongly reducing properties associated with acetylene flames caused by an abundance of fragments of the type C_2H, C_2, CH, etc. In particular, this could lead to significantly lower concentrations of free metal atoms, and despite their good signal-to-noise

ratios, hydrogen flames are less efficient at excitation and atomization, and exhibit more chemical interference with added analytes with respect to acetylene systems.

The temperature dependences of major product concentrations for three arbitrarily selected H_2/N_2O flames are shown in Figure 11, and the isothermal (2800K) fuel/oxidant ratio dependences of the concentrations of major species in Figure 12.

The temperature dependences of major product concentrations for H_2/O_2 flames are shown in Figure 13 for three arbitrarily chosen flame compositions, and the isothermal (2800K) distribution of products as a function of fuel/oxidant ratio in Figure 14.

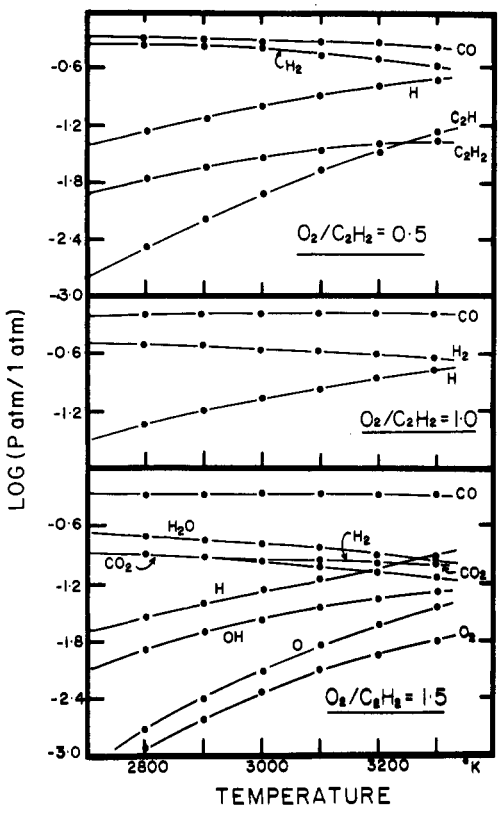

Figure 5. Temperature dependence of concentrations for major species generated in acetylene/oxygen flames at different fuel/oxidant ratios

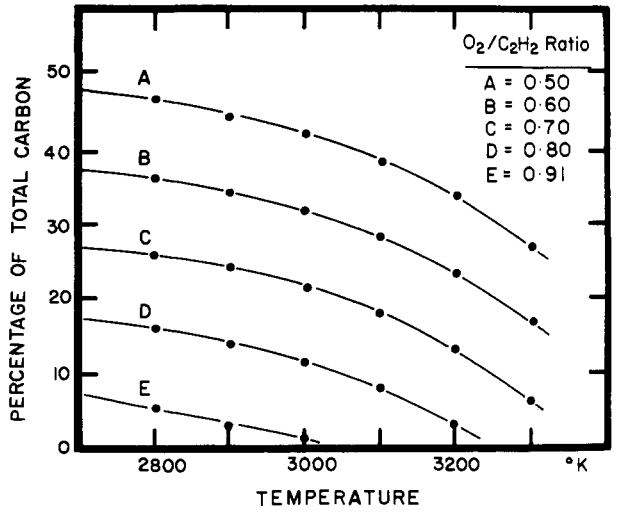

Figure 6. Temperature dependence of condensed carbon concentrations for different fuel/oxidant ratios in acetylene/oxygen flames

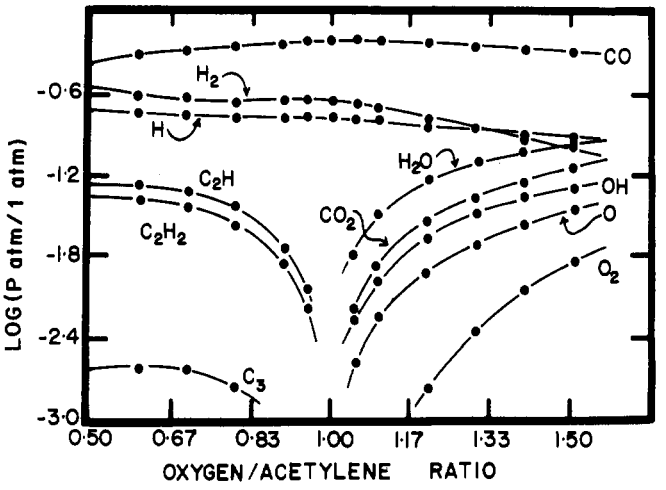

Figure 7. Dependence of concentrations for major species generated in acetylene/oxygen flames on the fuel/oxidant ratio under isothermal conditions (3300K)

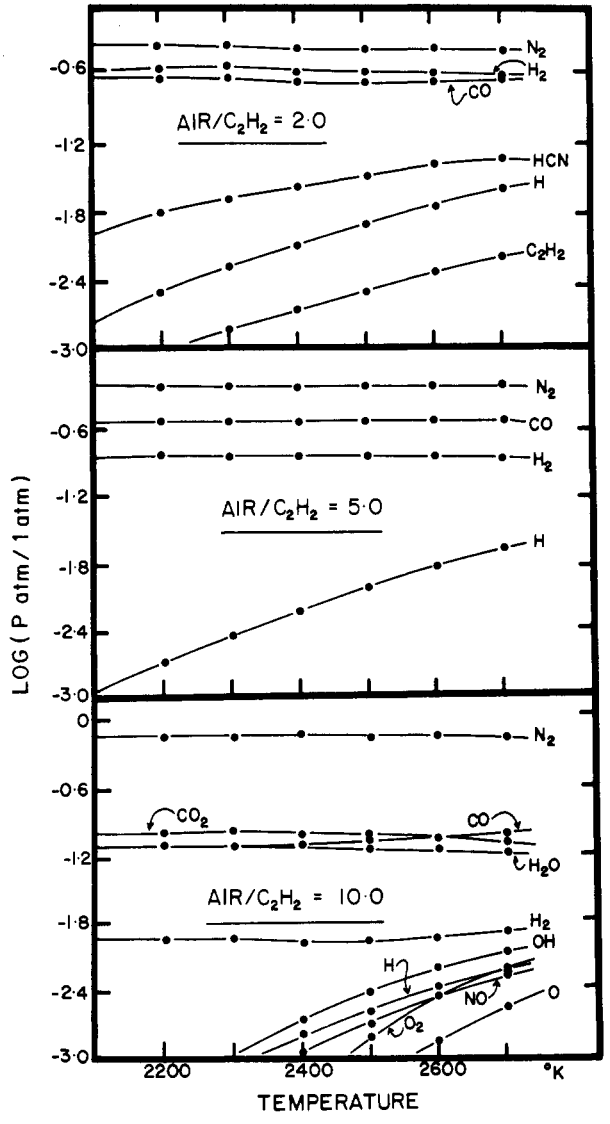

Figure 8. Temperature dependence of concentrations for major species generated in acetylene/air flames at different fuel/oxidant ratios

Hydrogen/air flames have a significantly lower temperature than the two considered above in this section, and this is reflected in the nature and abundance of the major species present. The temperature dependences of product concentrations are shown in Figure 15, and the isothermal (2300K) product concentrations as a function of fuel/oxidant ratio are given in Figure 16.

Discussion

Effects of stoichiometry on flame composition. After examination of the stoichiometry of hydrocarbon flames, this may be referred to CO production, or CO_2 production. Thus the terms fuel-rich or fuel-lean are relative. We will relate such references to CO production in the ensuing discussion.

Fragmentation of acetylene leads to formation of C_2H, C_2, CH, C, and H species. In fuel-rich flames one therefore expects a preponderance of such fragments in the absence of sufficient oxygen to form oxygen-containing entities. On the other hand, oxidant-rich flames would lead to the predomination of CO, CO_2, H_2O, OH, NO, and other such species. The calculations in this work support such prima-facie conclusions (Figures 1, 3, 5, 7, 8, and 10). Equally, it is apparent that as the flame becomes richer in hydrocarbon fuel content, significant fractions of the total carbon appear as solid condensed species (Figures 2, 6, and 9). Too much of this solid carbon in a flame renders it useless as a source for absorption and emission spectroscopy, since the analyte signals are masked by incandescence *(11)*. The diminution of reducing species as the oxidant content of the flame is increased is clearly demonstrated by the total disappearance of C_2H, C_2H_2, and CN from the list of principal products in intermediate N_2O/C_2H_2 flames and the sharp decrease in HCN content, followed by the rapid increase in O and OH concentrations as the oxidant/fuel ratio is

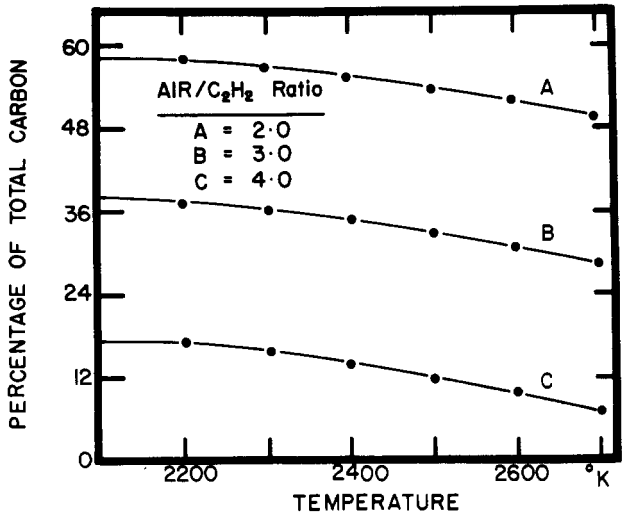

Figure 9. Temperature dependence of condensed carbon concentrations for different fuel/oxidant ratios in acetylene/air flames

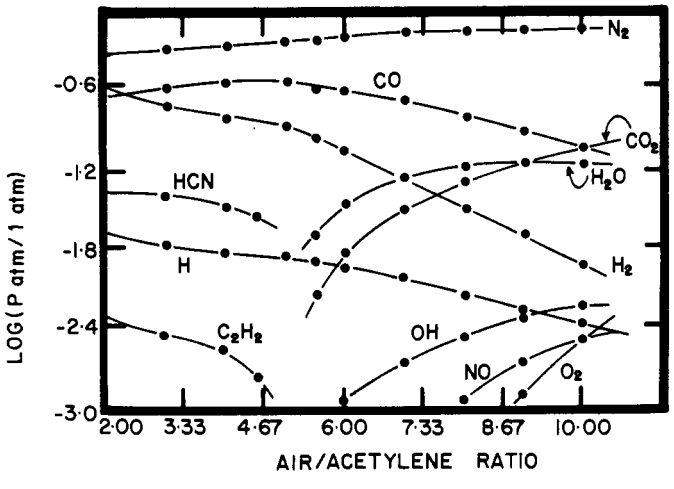

Figure 10. Dependence of concentrations for major species generated in acetylene/air flames on the fuel/oxidant ratio under isothermal conditions (2600K)

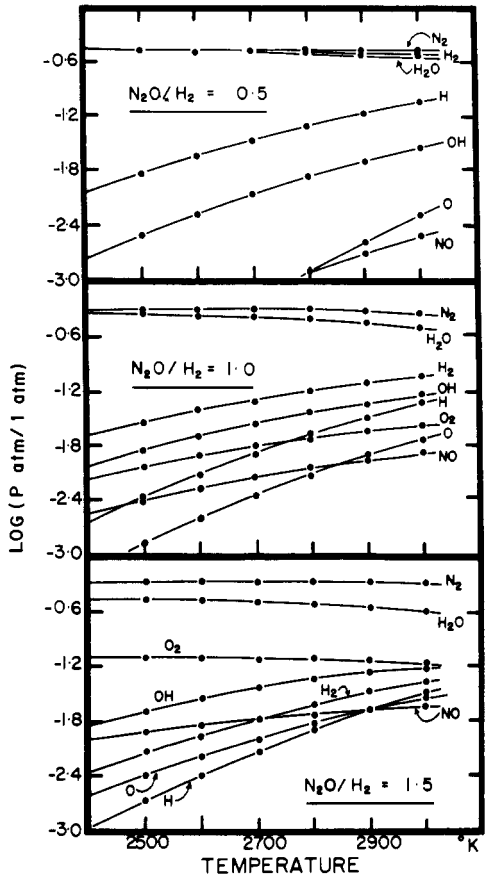

Figure 11. Temperature dependence of concentrations for major species generated in hydrogen/nitrous oxide flames at different fuel/oxidant ratios

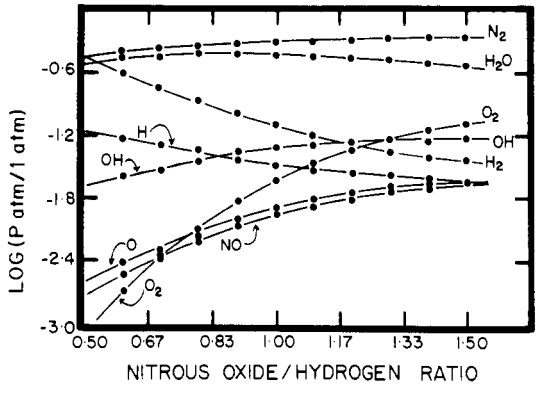

Figure 12. Dependence of concentrations for major species generated in hydrogen/nitrous oxide flames on the fuel/oxidant ratio under isothermal conditions (2900K)

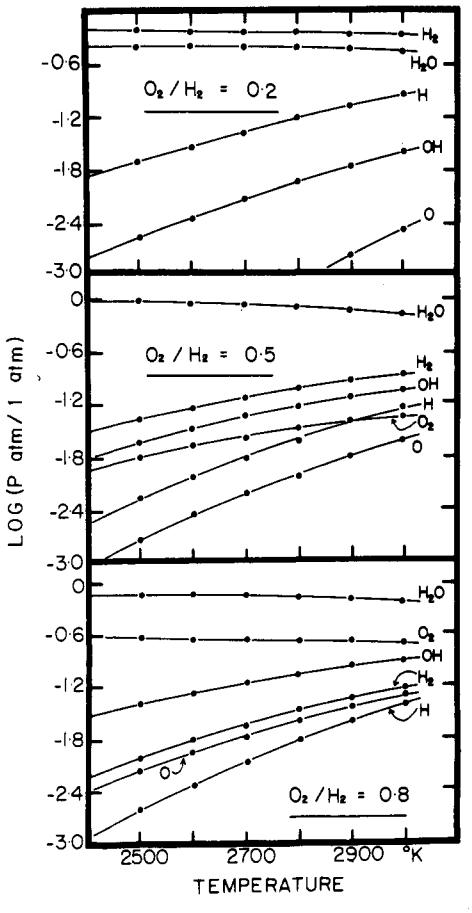

Figure 13. Temperature dependence of concentrations for major species generated in hydrogen/oxygen flames at different fuel/oxidant ratios

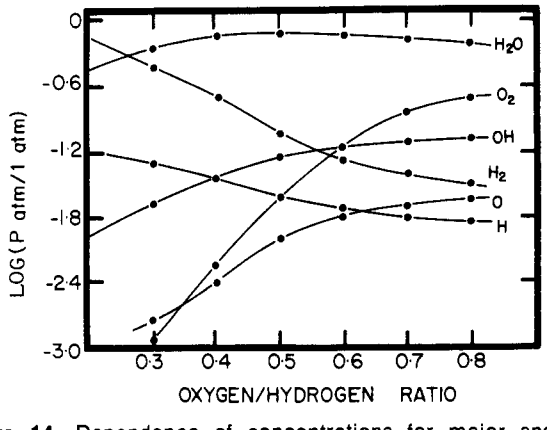

Figure 14. Dependence of concentrations for major species generated in hydrogen/oxygen flames on the fuel/oxidant ratio under isothermal conditions (2800K)

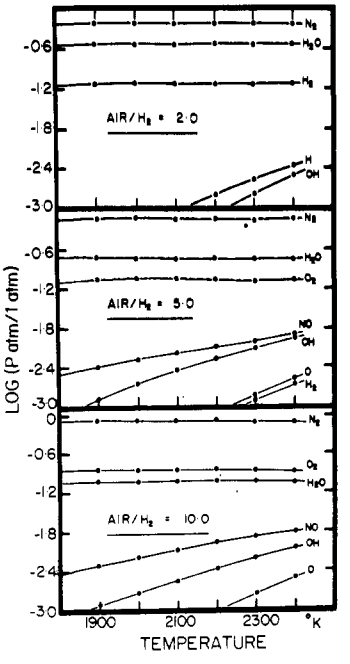

Figure 15. Temperature dependence of concentrations for major species generated in hydrogen/air flames at different fuel/oxidant ratios

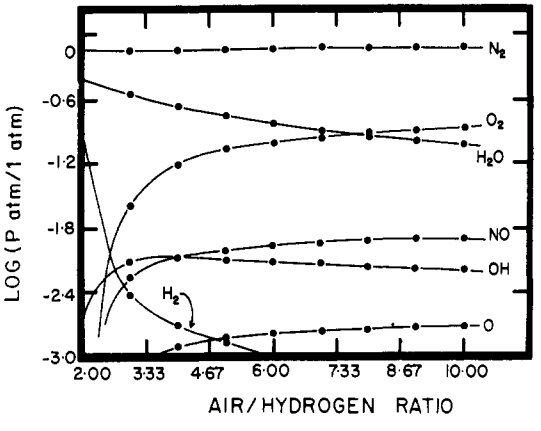

Figure 16. Dependence of concentrations for major species generated in hydrogen/air flames on the fuel/oxidant ratio under isothermal conditions (2300K)

increased still further. This relatively large abundance of O and OH makes these flames virtually useless for flame spectroscopy of elements that form refractory oxides. Also, a resulting chemiluminescence can mask the spectral region under observation and is attributed to such reactions as *(11)*:

$$CO + O \longrightarrow CO_2 + h\nu \qquad (7)$$

The only hydrocarbon fragment in the list of major products (Table I) for each of the three flame systems is C_2H, a direct reflection on the strength of the C—C bond (199.6 kcal/mol) in the acetylene fuel.

It is pertinent at this point to indicate that Taylor et al. in their calculations completely neglect any contribution from C_2H to the overall product distribution. From Table I it can be seen that this assumption is only valid for large ratios of N_2O/C_2H_2 (greater than 2.2). Equally large concentrations of unburnt fuel are present in fuel-rich flames, especially at the lower temperatures. The concentrations of C_2H in various flames directly reflect the temperatures accessible to the flame system; the higher the temperature, the greater the concentration of this species following increased thermal pyrolysis reactions. This latter effect leads to the total loss of C_2H as a major product from the C_2H_2/air system, which is probably ca. 300K lower in temperature compared to the C_2H_2/N_2O flame, and ca. 700K lower than the C_2H_2/O_2 flame. The isothermal plots of concentrations against C_2H_2/oxidant ratios (Figures 3, 7, and 10) demonstrate various concentration inversions—for example, the rise of CO concentrations to a maximum followed by a decline (Figure 10). These effects are plausibly attributed to secondary reactions be-

coming increasingly important. For example, it is inconceivable that CO_2 is formed in a single-step reaction.

Unlike hydrocarbon flames, where there is a choice of defining the stoichiometric reference, for hydrogen flames a stoichiometric ratio can only be defined in terms of H_2O production. In this context, intermediate ratio flames and stoichiometric flames are considered to be synonymous. As might be expected, the major product is water from all systems except where the quantity of uncombusted fuel—i.e., hydrogen—far exceeds the amount of combustion product—i.e., water. The concentration of OH in hydrogen flames is larger for oxygen-supported flames (as compared to N_2O-supported), and leads to an inferior signal-to-noise ratio in H_2/O_2 and H_2/air compared to H_2/N_2O systems. Further, the H_2/air flame differs substantially from the other two in that the system now contains large proportions of N_2, and is maintained at a much lower temperature. Introduction of N_2 leads to changes in product distribution, both qualitatively and quantitatively, although the N—N bond is of sufficient strength (225.8 kcal/mol) to prevent nitrogen-containing species from entering the major product listing with the sole exception of NO. The effects attributable to the lower overall temperatures manifest themselves in several ways. First, substantially lower OH concentrations result, and thus improved signal-to-noise ratios are obtained. On the other hand, the lower temperatures prevent adequate volatilization and atomization of certain metallic analytes thus introducing certain experimental limitations, but conversely, prevent ionization of free atoms which have low ionization potentials.

Stoichiometry effects on free-atom fractions. Data *(8, 12, 15, 18)* show that some free-atom fractions are markedly dependent on the fuel/oxidant ratio, whereas other metals are relatively unaffected. For example, Mo and Ti free-atom fractions are markedly enhanced by the use of fuel-rich flames. In contrast, Cu and Fe are relatively unaffected, and Al behaves in an intermediate fashion. The calculations presented here for Al, Cu, Fe, Mo, Si, Ti, and W (Figure 4) for C_2H_2/N_2O flames support these previous observations. Similarly, Taylor et al. *(3,4)* in their calculations found that Al and Si concentrations in particular were very sensitive to flame composition parameters. All metals examined, except Cu and Fe, showed an increase in free-atom fraction with a rise in temperature, a none-too-surprising result. On the other hand, Fe decreases slowly to a minimum and then begins to rise again; metal compounds formed in the flame show similar behavior. A rise in temperature, favoring the formation of endothermic species, is then counteracted beyond a certain temperature by increased fragmentation reactions. The fall in free-atom fractions as the oxidant content of system increases, which again is attributable to secondary reactions between elemental species and oxygen-bearing fragments, manifests itself in the increased formation of metallic oxides, hydroxides, and peroxides. This dramatic fall in free-atom fraction as the oxidant content increases is shown graphically in Figure 4. It is convenient (Equation 8) to refer to an enhancement factor in comparing free-atom fractions in fuel-rich flames to those in fuel-lean—i.e., oxidant-deficient—flames. Choosing two arbitrary ratios of N_2O/C_2H_2 at 1.80 (fuel-rich) and 2.20 (fuel-lean) we can define ϕ (enhancement factor) such that

$$\phi = \frac{\beta \text{ in fuel-rich flames}}{\beta \text{ in fuel-lean flames}} \qquad (8)$$

Since ϕ is a function of the relative concentrations of metallic oxides and other metallic, oxygen-bearing species, it should be dependent on the stability of the major metallic compound present—i.e., the metallic monoxide MO. Table II demonstrates the positive correlation between calculated enhancement factors and dissociation energies of the monoxide compounds for each of the elemental species examined. It seems apparent that fuel-rich hydrocarbon flames are to be preferred, since the abundance of reducing species (C_2H, CH, C_2, etc.) will lead to high concentrations of the free element, whereas fuel-rich hydrocarbon flames still contain appreciable quantities of oxygen-containing species. Although the metallic monoxide is the predominant species for the majority of systems considered it is not the only one contributing to changes in free-atom fractions. More importantly, the data calculated in Table III show that higher oxides, and certain other species, should *not* be ignored in these calculations, and that flame conditions should be chosen so as to minimize their formation.

Possible error sources. The calculations follow the methods described by White et al. *(16)* and Oliver et al. *(14)* and utilize a truncated Taylor's series (two terms) to express the set of mole numbers as an initial guess for the commencement of iteration. This will lead to a small but definite error in the absolute magnitude of any particular mole number, but should not interfere with the relative magnitudes to any great extent. In this work, we have not taken into account the fragmentation of solvents used to transport the analyte into the flame system. Since it is usual to use ethanolic solutions, or other organic materials, this could lead to an increase in carbon-containing fragments, and so increase the relative reducing nature of the flame atmosphere. However, Lvov *(6)* found that the solvent did not drastically alter the flame composition, and in view of the fact that aspiration rates rarely exceeded milliliters per minute magnitude flow rates, whereas the combustants are supplied at the order of several liters per minute, this is not surprising. Regarding the analyte itself, we have not taken account of ionization processes in calculating free-atom fractions, but as the ionization potentials of the elements considered (except Al and Ti) were in excess of 7 eV, this will not greatly affect the calculations of free-atom fractions reported here. Finally, it is suggested that a slightly different experimental basis might lead to equally consistent and perhaps more significant results. The experimental

Table II. Calculated Enhancement Factors, for Free-Atom Fractions in Nitrous Oxide/Acetylene Flame Systems at 2900K at Two Arbitrarily Chosen Oxidant/Fuel Ratios, as a Function of the Dissociation Energy of the Monoxide Species

Element	Calcd enhancement factor[a,b], (ϕ)	Dissociation energy of monoxide (9), eV
Cu	1	4.1 ± 0.3
Fe	1	4.3 ± 0.5
Al	2	4.6 ± 0.1
Mo	70	5.0 ± 0.7
Ti	2,000	7.2 ± 0.1
W	7,000	6.8 ± 0.4
Si	10,000	8.1 ± 0.3

[a]See text for definition. [b]Fuel-rich mixtures N_2O/C_2H_2 ratio of 1.80, fuel-lean mixtures N_2O/C_2H_2 of 2.20.

Table III. Calculated Mole Fractions of Compounds Formed by Added Elemental Species in Nitrous Oxide/Acetylene Flames at 2900K for Different Oxidant/Fuel Ratios[a]

Element, M	N_2O/C_2H_2 ratio	Species formed						
		M	MH	MO	MO_2	MO_3	M_2O_6	MOH
Al	1.90	0.9749	0.0251					
	2.00	0.9740	0.0222					0.0038
	2.10	0.6996	0.0173	0.0621				0.2210
Cu	1.90	1.0000						
	2.00	1.0000						
	2.10	0.9986		0.0014				
Fe	1.90	1.0000						
	2.00	1.0000						
	2.10	0.9920		0.0080				
Mo	1.90	0.9999		0.0001				
	2.00	0.9986		0.0014				
	2.10	0.0629		0.0359	0.8441	0.0571		
Si	1.90	0.4055	0.0004	0.5941				
	2.00	0.0224		0.9776				
	2.10	0.0001		0.9991	0.0008			
Ti	1.90	0.8905		0.1095				
	2.00	0.3561		0.6439				
	2.10	0.0012		0.9988				
W	1.90	0.9527		0.0473				
	2.00	0.6719		0.3265	0.0016			
	2.10	0.0006		0.2089	0.6847	0.1056	0.0002	

[a]Ratios chosen to be close to critical region as demonstrated by Figure 4.

assumptions made were that the flame system be regarded as an equilibrium closed adiabatic system, and that for this essentially static system, the thermostatic criteria of minimum free-energy attainment be applied. However, it is suggested that the flame system is probably better regarded as a living dynamic system, and thus subject to the thermodynamic (as opposed to thermostatic) criteria of nonequilibrium methods involving the minimum production of entropy as the criteria of equilibrium in dynamic processes.

Nomenclature

X = $X(x_1, x_2, \ldots x_i \ldots)$, a nonnegative set of mole numbers

x_i = mole number for the ith species

Z_i = corrected mole number derived from x_i to allow for negative values of x_i generated in the iteration process

$G(X)$ = Gibbs free energy of the system

μ_i = chemical potential of the ith species

μ_i° = standard chemical potential for the ith species

a_{ij} = number of atoms of type j in the ith chemical species

b_j = total number of atomic weights for atom type j in the original flame mixture

Δ = an arbitrarily set difference parameter defining the end of the iteration process

P, T, R = total pressure, temperature on the absolute scale of the system, and gas constant/mol, respectively.

Literature Cited

(1) Anderson, C. H., presented at Pittsburgh Conference on Analytical Chemistry and Applied Spectroscopy, Cleveland, Ohio, March 1968.
(2) Brinkley, S. R., *J. Chem. Phys.*, **15**, 107 (1947).
(3) Chester, J. E., Dagnall, R. M., Taylor, M. R. G., *Anal. Chim. Acta*, **51**, 95 (1970).
(4) Chester, J. E., Dagnall, R. M., Taylor, M. R. G., *ibid.*, **55**, 47 (1971).
(5) Dean, J. A., Rains, T. C., "Flame Emission and Atomic Absorption Spectrometry," p 202, Marcel Dekker, New York, N.Y., 1969.
(6) Dean, J. A., Rains, T. C., "Flame Emission and Atomic Absorption Spectrometry," p 326, Marcel Dekker, New York, N.Y., 1969.
(7) Denbigh, K. G., "The Principles of Chemical Equilibrium," 2nd ed., p 115, Cambridge University Press, Cambridge, England, 1966.
(8) Fassell, U. A., Rasmuson, J. O., Kniseley, R. N., Cowley, T. G., *Spectrochim. Acta*, **25B**, 559 (1970).
(9) Gaydon, A. G., "Dissociation Energies and Spectra of Diatomic Molecules," 3rd ed., Chapman and Hall, London, England, 1968.
(10) JANAF Thermochemical Tables, Dow Chemical Co., 1965–1968.
(11) Kirkbright, G. F., Peters, M. K., West, T. S., *Talanta*, **14**, 789 (1967).
(12) Kniseley, R. N., Butler, C. C., Fassell, V. A., *Anal. Chem.*, **41**, 1494 (1969).
(13) Krieger, F. J., White, W. B., *J. Chem. Phys.*, **16**, 358 (1948).
(14) Oliver, R. C., Stephanon, S. E., Baier, A. W., *Chem. Eng.*, 121 (Feb. 19, 1962).
(15) Pickett, E. E., Khoirtyohann, S. R., *Spectrochim. Acta*, **2313**, 235 (1968).
(16) White, W. B., Johnson, S. M., Dantzig, G. B., *J. Chem. Phys.*, **28**, 751 (1958).
(17) Willis, J. B., Fassell, U. A., Fiorino, J. A., *Spectrochim. Acta*, **24B**, 157 (1969).
(18) Willis, J. B., Rasmuson, J. O., Kniseley, R. N., Fassell, V. A., *Spectrochim. Acta*, **23B**, 725 (1968).

Received for review April 6, 1972. Accepted September 28, 1972. Data in this paper were taken from work submitted by L. L. R. to the Graduate School of West Virginia University in partial fulfillment of the requirements for the MS degree. Full details of all calculations may be obtained from the MS thesis of L. L. R., W. V. U., Morgantown, 1970. We thank The Research Corp. for partial support of this project.